Hot carbon fiber acoustic vector sensor and flowmeter with simple and low cost fabrication method

mehdi abedi[1], avazpour[2], and abbasi[2]

[1]Yasuj University
[2]Affiliation not available

February 21, 2019

Abstract

In this paper, a new type of hot wire acoustic vector sensor based on Polyacrylonitrile base carbon fiber, as a sensing element is presented. The vector sensor employs two suspended carbon fiber with micro size diameter and millimeter length as a pair of hot wires that are close together with hundreds micron separation. V-I and V-R curves shows that temperature coefficient resistivity is negative for carbon fibers. Sensitivity of the sensor has been measured with different bias voltage that shows either the direction of the air flow or the acoustic source would be detected by comparing the output voltages of two suspended carbon fibers.

Keywords: hot wire; carbon fiber; thermoresistive; low frequency acoustic vector sensor

Introduction

Today, the thermo-resistive effect is an attractive phenomenon in the field of micro and nano electro mechanical system (MEMS and NEMS) and sensors manufacturing. Because of the MEMS technology developments, the vector sensors have progressed a lot . In particular, in the field of acoustic sensors, there is a lot of research to replace conventional array with acoustic vector sensors(AVSs). In general a conventional acoustic array employs multiple scaler sensors for signal enhancement, source localization, target tracking ,etc(Nehorai and Paldi 1994; Hochwald and Nehorai; Zou and Nehorai 2009; Hawkes and Nehorai 2003)(Nehorai and Paldi 1994; Hochwald and Nehorai; Zou and Nehorai 2009; Hawkes and Nehorai 2003). Some of the key aspects of an AVS are its small size, low weight and ability to determine the acoustic pressure and the particle velocities simultaneously. Benefits from these properties, AVS tends to be more attractive for exploitation and commercialization than conventional sensor array(Cao et al. 2017). Hot wire(HW) AVSs which have been used for more than decades, typically have been made of two Pt or tungsten micro wires(Wang et al. 2017). They have hundreds of micron length and about 5 microns in diameter and distance of tens microns from each other. HWAVSs are used for frequency and source level (SL) measurement and also for direction finding of the acoustic source.

HWAVSs same as Microflown consist of two or more very closely spaced bridges of silicon nitride with platinum electrodes(Jacobsen and de Bree 2008)(details can be found in http://www.microflown-avisa. com/).

However, the fabrication of these sensors, which requires expensive materials, clean room facilities and specialized wafer processing equipment, has increased their cost, especially for small-scale production(Nguyen et al. 2014; Hung et al. 2000). Moreover, the fabrication of thermal flow sensors has involved various solvents and chemicals which are unfriendly for the environment and could lead to contamination issues. In addition,

these sensors are unable to work in harsh conditions such as high temperature and corrosive environments. Therefore, there is a high demand for investigating alternative novel thermal sensing materials for advanced thermal sensors. Desirable characteristics of these sensors would be (1) low cost and high sensitivity, (2) linear response, stability and sustainability, (3) capability of working in harsh environments such as at high temperatures and (4) flexibility and suitability for a wide range of applications, including the emerging field of wearable applications(Dinh et al. 2017).

Therefore, there is a high demand to investigate the low cost and environmentally friendly materials for thermal sensors[16]. Carbon fibers (CFs)can be a good material for this purpose because of its ubiquitousness and relatively high temperature coefficient of resistance (TCR)(Donnet et al. 2003).

Carbon nanotubes(CNTs) and CFs which possess remarkable mechanical, thermal and electrical properties, have been widely utilized for sensing in many applications such as motion control, temperature sensor and flow measurement(Donnet et al. 2018). Most efforts have been focused on exploring the applications of an individual CNT, bulk or bundled CNT and CF have rarely been involved in the researches.

CFs are fibrous carbon materials with carbon content more than 90%. They are transformed from organic matter by 1000 – 1500°C heat treatment, which are the substance with imperfect graphite crystalline structure arrange along the fiber axis. The existence of carbon fiber came into being in 1879 when Edison took out a patent for the manufacture of carbon filaments suitable for use in electric lamps. CFs have attractive properties, such as strength, good electrical conductivity, stability on exposure to reactive media, low density, low-to negative coefficient of thermal expansion, and resistance to shock heating. The most representative applications of CFs are as sorption materials, electrostatic discharge materials, catalysts, and reinforcement materials in composites.

Some CF classifications are based on CF modulus, strength, and final heat treatment temperature. Based on precursor fiber materials, CNFs are classified into: Polyacrylonitrile (PAN)-based, Pith-based, Mesophase pith-based, Isotropic pitch-based, Rayon-based, Gas-phase-grown CFs.

The characteristics of CF material are influenced by choices of the initial polymer raw material, conditions of carbonization and heat treatment, and also by introduction of certain additives. PAN-based CNFs demonstrate 200 – 400 GPa Young's modulus upon longitudal stretching of the fiber, mesophase pitch-based CNFs are at interval 150 – 800 GPa. CFs have much higher heat resistance than many other known materials. The maximum temperature in air at which the structural and mechanical characteristics still remain unaltered is 300°C. The electrical properties of CFs are explained in terms of π-electron delocalization. It is known that percoalion occurs due to tunneling or hopping of electrons from one fiber to other fiber or by actual formation of a nanofiber network. Variations in composition and structure of CNFs, related to the conditions of their production and to impurities present in their structure, are the cause of changes in electrical resistivity of these materials, resulting in properties ranging from those of conductors to semiconductors(Donnet et al. 2003).

Materials and Methods

We used a PAN-based CF instead of Pt or other metals for fabrication of our HW sensor. The electrical resistance, R, of a fiber with length can be calculated with the following formula[18]:

$$R = \rho \frac{l}{A} = \rho \frac{4l}{\pi d^2}$$

Where R is the resistance of the fiber [], $l$is the length of the fiber [m], ρ is the electrical resistivity of fiber

[. m], A is the cross-sectional area [m2], d is the nominal diameter of the fiber [m]. Electric resistivity, , is a measure of how strongly a wire opposes electric current[18].

Hot CF AVS (HCFAVS) is an electromechanical system that is based on the change of the electrical resistivity of fiber with changing CF temperature

$$\rho(T) = \rho_0 (1 + \alpha (T_{CF}(P) - T_r))$$

Where T_r is the electrical resistivity at room temperature , T_{CF} is the average temperature in the CF and depends to electrical power, P or bias voltage, α is the thermal resistance coefficient (TCR) of CF. Details of this discussion are given in reference [13].

Flow rate is measured by sensing of changes in heat transfer from electrically heated wires exposed to the fluid. Flow direction is determined from amount of heat transfer between wires and fluid.

Experimental Details

Sensor fabrication

The T300 CF that has been used experimentally in our research, is made by Toray CFs Company. The diameter of the CF is $7\mu m$. Two suspended fibers are used to make the sensor, each of which is at one side of printed circuit board (PCB) and at a distance equal to PCB thickness. PCB consists of an insulating layer in the middle and two layers of copper on both sides. The thickness of the PCB is between "100-200" . To improve the quality of suspended CF (SCF) bonding, silver glue has been used at its two ends. This is done manually using a microscope and to prevent the breakdown of SCFs due to tensions and mechanical oscillations of PCBs, we have placed it between two insulating flat plates. The schematic image of sensor is shown infigure 1. Reference resistors are used to measure the changes in the SCFs current by converting the current variations to voltage variations. What is measured by an oscilloscope is the voltage difference between the two sides of the reference resistors in AC and DC mode.

For testing of contacts quality, electrical resistance of each CF on two side of PCB was measured by a multimeter at room temperature.

We have investigated the self-heating problem through a separate measurement of the voltage-current diagram for each SCF. Figure 2 shows that with increasing bias voltage of a single SCF and occurrence of self-heating phenomenon at higher voltage, the SCF's resistance decreases, which means that the temperature coefficient of resistance (TCR) of the SCF is negative. Reduction of SCFs resistance under various degrees of applied electrical power is shown in Figure 2(c). In Figure 2(d), the results of the simultaneous increase of the bias voltage for two CFs in a sensor are shown. The initial electrical resistance of the SCFs is different, but the slope of the changes is the same.

Results and Discussion

Sensor response to air flow:

We have investigated the problem of sensor response to air flow and its steady state performance in a wind tunnel for flow velocity from 0-2 m/s which was measured also by an anemometer. The fabricated sensor was operated in constant bias voltage mode. Two constant voltage power supply have been used for SCFs biasing in a fixed voltage and then current variation (drop) of each SCF A and B have been recorded at

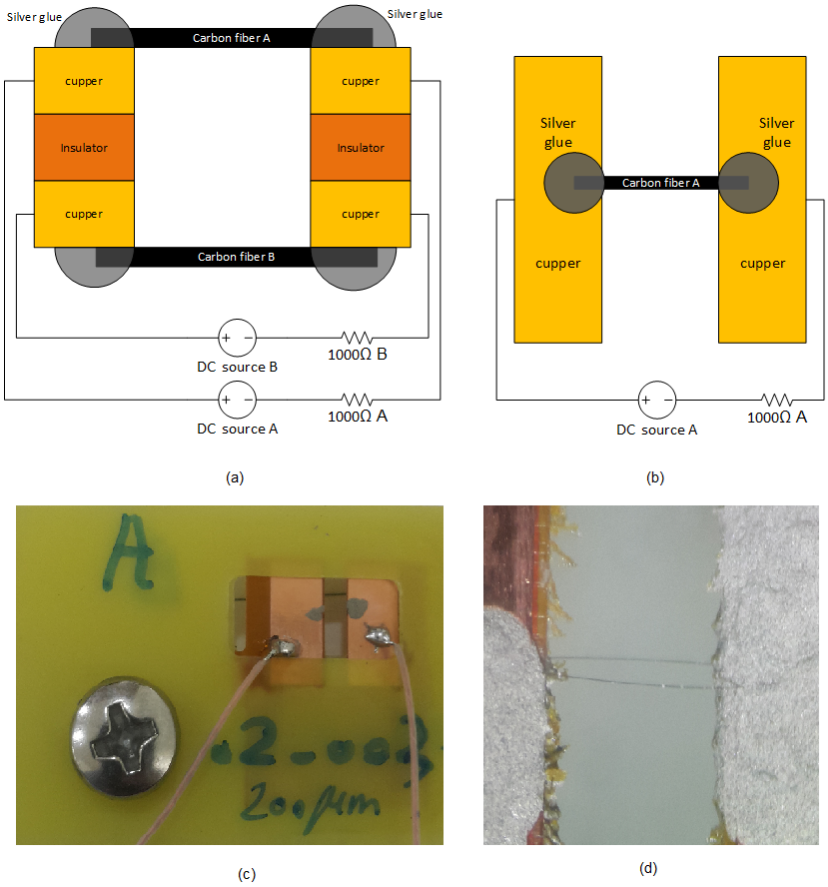

Figure 1: Schematic and real image of sensor: (**a**) Sensor view from the top. Reference resistors are used to measure the changes in the sensor current by converting the current variation to voltage. What is measured by an oscilloscope is the voltage difference between the two sides of the reference resistors in AC and DC mode; (**b**) Sensor -side view schematic; (c) real Sensor -side view; (d) an image of the SCFs under the microscope.

different air velocity condition. Figure shows the steady state characteristics of HCFAVS for flow velocity from 0. 5 – 2 m/s. Due to negative TCR of CF the current across the SCFs decreases as the flow rate increases and according to Figure 3 they have linear relation in the range of 0. 5- 2 m/s flow rate. Direction of flow can be determined by comparison of current variation of two SCFs, A and B. In this experiment the flow direction has been on the side of SCF B because of its larger current variation.

Sensor response to Acoustic wave:

A speaker attached to a tube with 35 cm length and 6. 5 cm diameter and a signal generator have been used for acoustic wave generation with different acoustic SL at different frequencies. HCFAVS is placed at the other end of the tub and before the main test, SL of speaker was determined by a SL Meter at this point. Figure 4 shows the schematic of experimental setup.

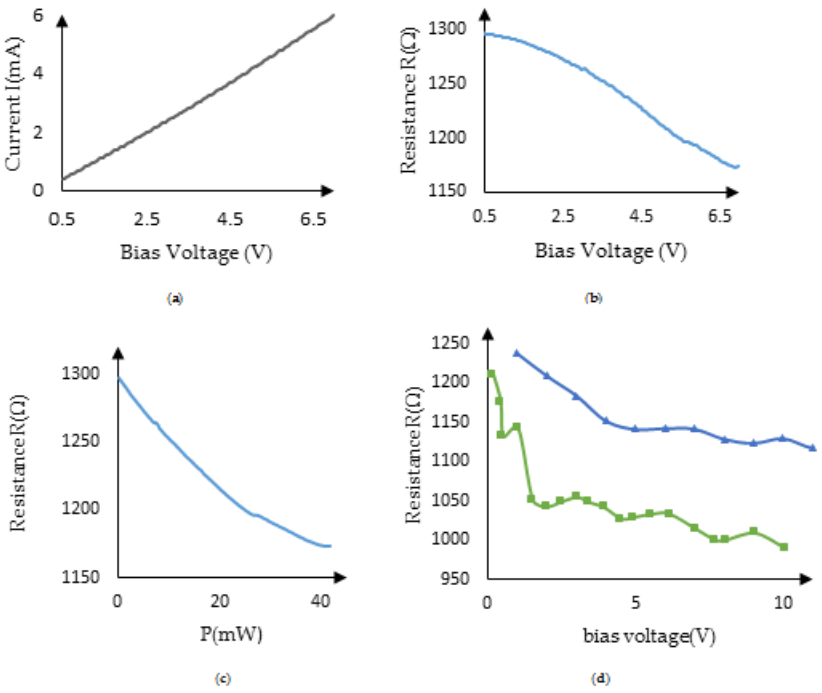

Figure 2: (a) V-I curve of a SCF; (b) V-R curve of a SCF; (c) P-R curve of a SCF; (d)V-R curve for two SCFs A (green curve) and B (blue curve) in a sensor This is a caption

Direction of acoustic source

To determine the direction of the audio source, the output variation (decrease) of each fiber is compared. Due to the negative value of TCR, acoustic wave decreases the fiber temperatures and then their resistance increases and the amount of electric current decreases. The fiber that is located on the audio source side is experiencing a higher temperature drop, resulting in larger output changes. Its mean value of output signal also is less than the other fiber (SCF A). Figure 5 shows the output signal of A (red) and B (green) SCFs. The figure shows that the source is on the B SCF side because the mean value of B SCF signal is less than A and also its output variation is larger than A SCF.

Sensitivity of sensor to bias voltage

Sensitivity of sensor relative to bias voltage was measured and experiments have been shown that for 150 Hz acoustic wave with 90 dB SL at the sensor point, increasing of bias voltage of every SCFs increases the output signal. Figure 6 shows the output of sensor for different bias voltage of SCFs.

We have also investigated the interaction of each micro-wire on each other and its effect on acoustic sensitivity. The sensitivity (output signal) of one of the micro-wires was measured as a result of variations in the bias of another micro-wire from 0 to allowed voltage. When the bias voltage of one of the SCFs is equal to zero, it means that we have a sensor with a single SCF, and in this case we see the lowest output signal level in the other SCF. Experiment shows that it has minimum sensitivity and by increasing the bias voltage of SCF B, sensitivity of SCF A has been increased. Figure 7 shows normalized variation of SCF A output according to bias voltage of SCF B. Figure 8 shows output signals and wave forms of SCF A and B and their difference

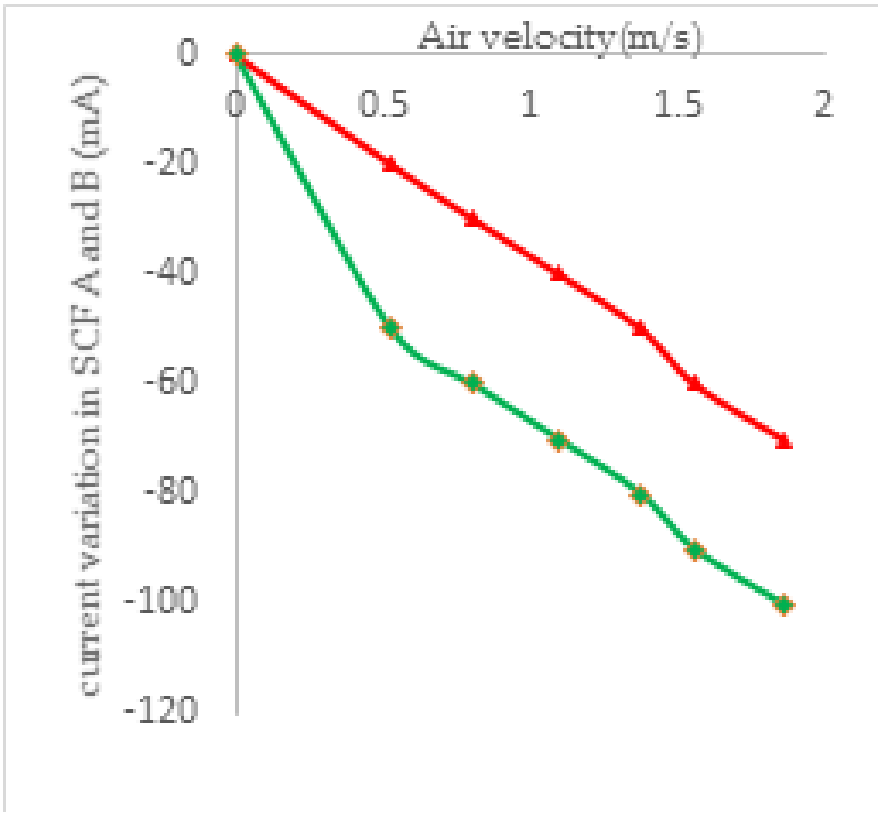

Figure 3: Steady state characteristics of HCFAVS for air velocity from 0 – 2 m/s. red curve is for SCF A and green curve is for SCF B. Reducing the electric current in the SCF B is more than the SCF A, so the direction of the air flow has been on the SCF B side.

on oscilloscope. In this experiment acoustic frequency was 150 Hz with 90 dB SL.

Conclusions

We show that fabrication of HCFAVS is very simple and low cost in comparison with Pt HWAVS, especially for small-scale production. We determined the sign of TCR for the CFs used in our experiments by investigating the effect of self-heating, and it was found that its sign is negative, and this is consistent with other references. We determined the I-V characteristics of the CF HWAVS for investigating the self-heating phenomenon. Sensor sensitivity investigated for different bias voltage of SCFs. We have also investigated the interaction of each SCF on each other and its effect on acoustic sensitivity. We show that fabricated sensor can be used as a vector DC flow meter with good sensitivity to air velocity and its direction. At the end, it was shown that our sensor can be used as a low-frequency AVS.

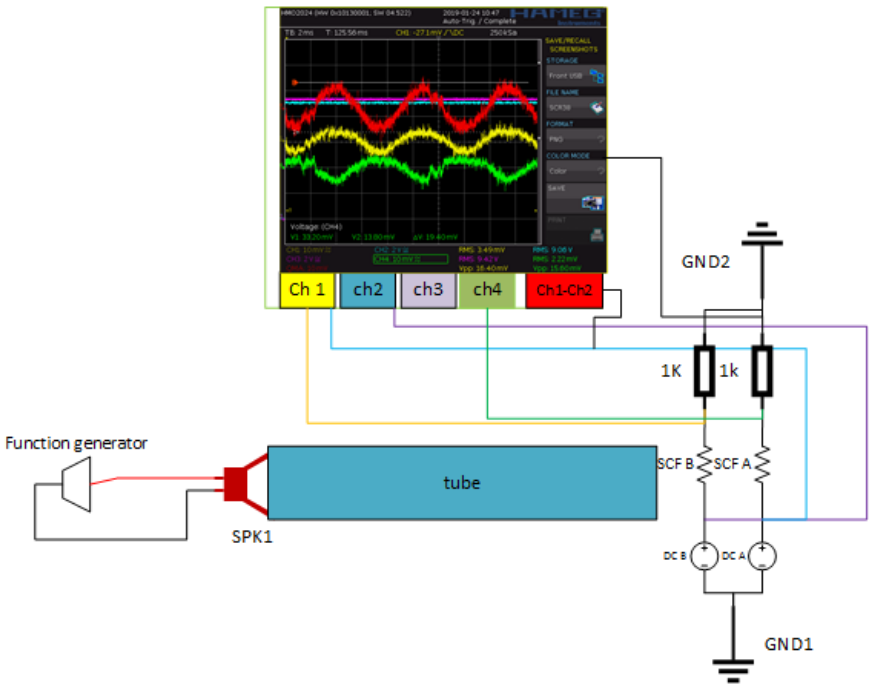

Figure 4: Schematic of experimental setup for investigation of sensor response to an acoustic wave

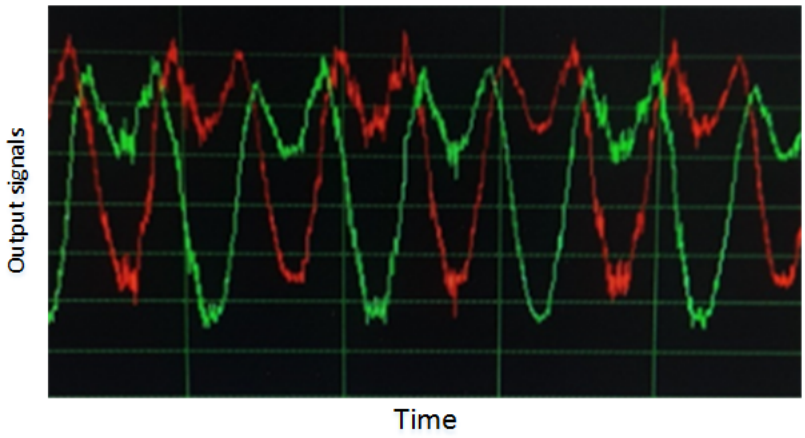

Figure 5: Output signal of A (red curvature) and B (green curvature) SCFs. It is obvious that variation of SCF B is more than SCF A

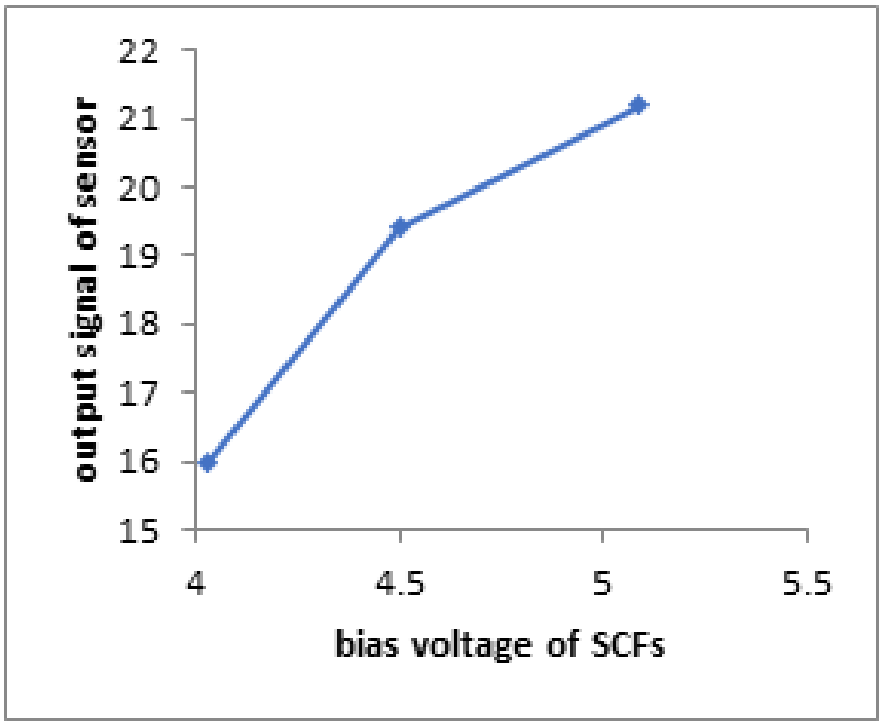

Figure 6: Bias voltage of SCFs of a sensor

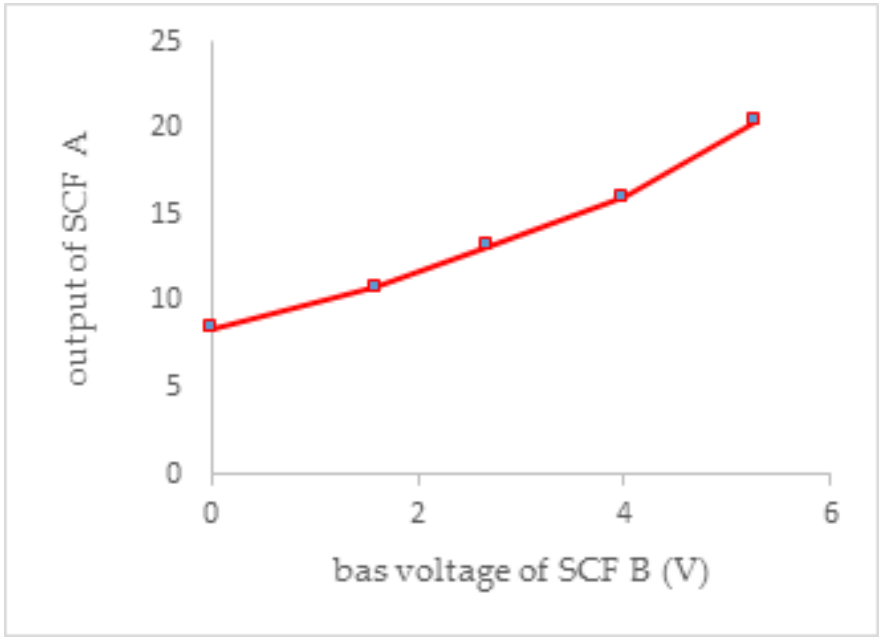

Figure 7: Normalized variation of SCF A output according to bias voltage of SCF B

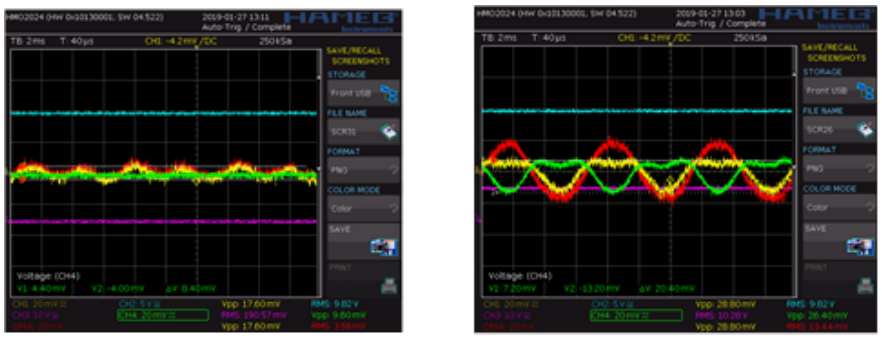

(a) (b)

Figure 8: Investigation of effect of SCF B bias voltage on sensitivity of SCF A. Output variation of SCF A and B due to an acoustic wave (150 Hz with 90 dB SL), with different bias voltage of SCF B: (**a**) Bias of SCF B is 0 V (green curve) and output variation of SCF A (yellow curve), and red curve shows yellow curve mines green curve; (**b**) Bias of SCF B is 5. 26 V and variation of its output (green curve), and output variation of SCF A (yellow curve), and red curve shows yellow curve mines green curve.

References

Cao J, Liu J, Wang J, Lai X (2017) Acoustic vector sensor: reviews and future perspectives. IET Signal Processing 11:1–9. doi: 10.1049/iet-spr.2016.0111

Dinh T, Phan H-P, Qamar A, and others (2017) Thermoresistive Effect for Advanced Thermal Sensors: Fundamentals Design Considerations, and Applications. Journal of Microelectromechanical Systems 26:966–986. doi: 10.1109/jmems.2017.2710354

Donnet J-B, Bansal RC, Wang M-J (2018) Carbon Black. Routledge

Donnet JB, Bahl OP, Bansal RC, Wang TK (2003) Carbon Fibers. In: Encyclopedia of Physical Science and Technology. Elsevier, pp 431–455

Hawkes M, Nehorai A (2003) Wideband source localization using a distributed acoustic vector-sensor array. IEEE Transactions on Signal Processing 51:1479–1491. doi: 10.1109/tsp.2003.811225

Hochwald B, Nehorai A Identifiability in Array Processing Models with Vector-Sensor Applications. In: IEEE Seventh SP Workshop on Statistical Signal and Array Processing. IEEE,

Hung S-T, Wong S-C, Fang W (2000) The development and application of microthermal sensors with a mesh-membrane supporting structure. Sensors and Actuators A: Physical 84:70–75. doi: 10.1016/s0924-4247(99)00358-1

Jacobsen F, de Bree H-E (2008) The Microflown Particle Velocity Sensor. In: Handbook of Signal Processing in Acoustics. Springer New York, pp 1283–1291

Nehorai A, Paldi E (1994) Acoustic vector-sensor array processing. IEEE Transactions on Signal Processing 42:2481–2491. doi: 10.1109/78.317869

Nguyen HB, Mailly F, Latorre L, Nouet P (2014) A new monolithic 3-axis thermal convective accelerometer: principle design, fabrication and characterization. Microsystem Technologies 21:1867–1877. doi: 10.1007/s00542-014-2254-0

Wang D, Xiong W, Zhou Z, and others (2017) Highly Sensitive Hot-Wire Anemometry Based on Macro-Sized Double-Walled Carbon Nanotube Strands. Sensors 17:1756. doi: 10.3390/s17081756

Zou N, Nehorai A (2009) Circular Acoustic Vector-Sensor Array for Mode Beamforming. IEEE Transactions on Signal Processing 57:3041–3052. doi: 10.1109/tsp.2009.2019174